

PROCEEDINGS OF SPIE

[SPIDigitalLibrary.org/conference-proceedings-of-spie](https://spiedigitallibrary.org/conference-proceedings-of-spie)

Multiplication-based analog motion detection chip

Andrew J. Moore, Christof Koch

Andrew J. Moore, Christof Koch, "Multiplication-based analog motion detection chip," Proc. SPIE 1473, Visual Information Processing: From Neurons to Chips, (9 July 1991); doi: 10.1117/12.45542

SPIE.

Event: Orlando '91, 1991, Orlando, FL, United States

A multiplication based analog motion detection chip

Andrew Moore
Christof Koch

Computation and Neural Systems Program
California Institute of Technology MS 216-76
Pasadena, CA 91125

ABSTRACT

A novel use of an analog motion detection circuit is presented. The circuit, developed by Tanner and Mead¹⁻³ computes motion by dividing the time derivative of intensity by its spatial derivative; the four quadrant division is realized with a multiplier within a negative feedback loop. We have opened the loop, and characterized the circuit as a multiplication-based motion detector, in which the output is the product of the temporal and spatial derivatives of intensity, for various light levels and various moving patterns. An application to the time-to-contact computation is presented.

1. INTRODUCTION

Visual motion detection strategies rely on feature correlation or the manipulation of the derivatives of intensity. The Tanner-Mead optical motion detector circuit¹⁻³ implements the “gradient model” of motion detection, in which the ratio of the temporal derivative to spatial derivative is computed. Since the circuit is built in subthreshold analog VLSI technology, with light sensors and computing elements on the same chip, it represents a low-power, compact means to measure motion.

The Tanner-Mead detector was originally tested for idealized visual inputs. Our goal was to put a lens on the chip and point it at moving patterns under a variety of conditions; ultimately, we hoped to test the circuit in a time-to-contact computation. In short, we achieved our goal, but in an unexpected way. Faced with intensity signals that varied over a large range, we tuned the circuit in a way that could cope with the range, and analysis of the performance indicates that the chip tuned in this manner is not dividing the derivatives but multiplying them. Still, the circuit is useful for measuring the motion of a class of patterns.

In the following, we describe the motion detection circuit, characterize its performance in a novel operating mode, and demonstrate its use in a time-to-contact scenario.

2. THE TANNER-MEAD MOTION DETECTION CIRCUIT

2.1 Theory of operation

The gradient model of motion estimation relies on the assumption that the total derivative of intensity over time does not change⁴. This total derivative, expanded to partials, yields an expression involving velocity and the temporal and spatial derivatives of intensity:

$$\frac{dI}{dt} = I_x v + I_t = 0, \quad (0.1)$$

where I is intensity, I_x and I_t are the spatial and temporal derivatives of intensity, and v is velocity. Solving for v , we have

$$v = -\frac{I_t}{I_x}. \quad (0.2)$$

In analog circuitry, there is no way to divide two signed quantities directly. Instead, a multiplication of the quantities must be situated within a negative feedback loop. In the Tanner-Mead motion detector, the following relation is implemented:

$$(I_x v + I_t) I_x = \epsilon \mapsto 0. \quad (0.3)$$

When the error ϵ is minimized, the velocity is the correct ratio of derivatives. The second multiplication by I_x eliminates the singularity that would otherwise result when $I_x = 0$, i.e., when there is no detail in the scene.

2.2 Circuit implementation

The circuit for motion detection is shown in Figure 1. The photoreceptors are built from phototransistors (shown as a current source, bottom left) pulling down on a stack of two diodes. The time derivative is taken by feeding the input and output of a follower-integrator to a differential pair (labeled I_t).

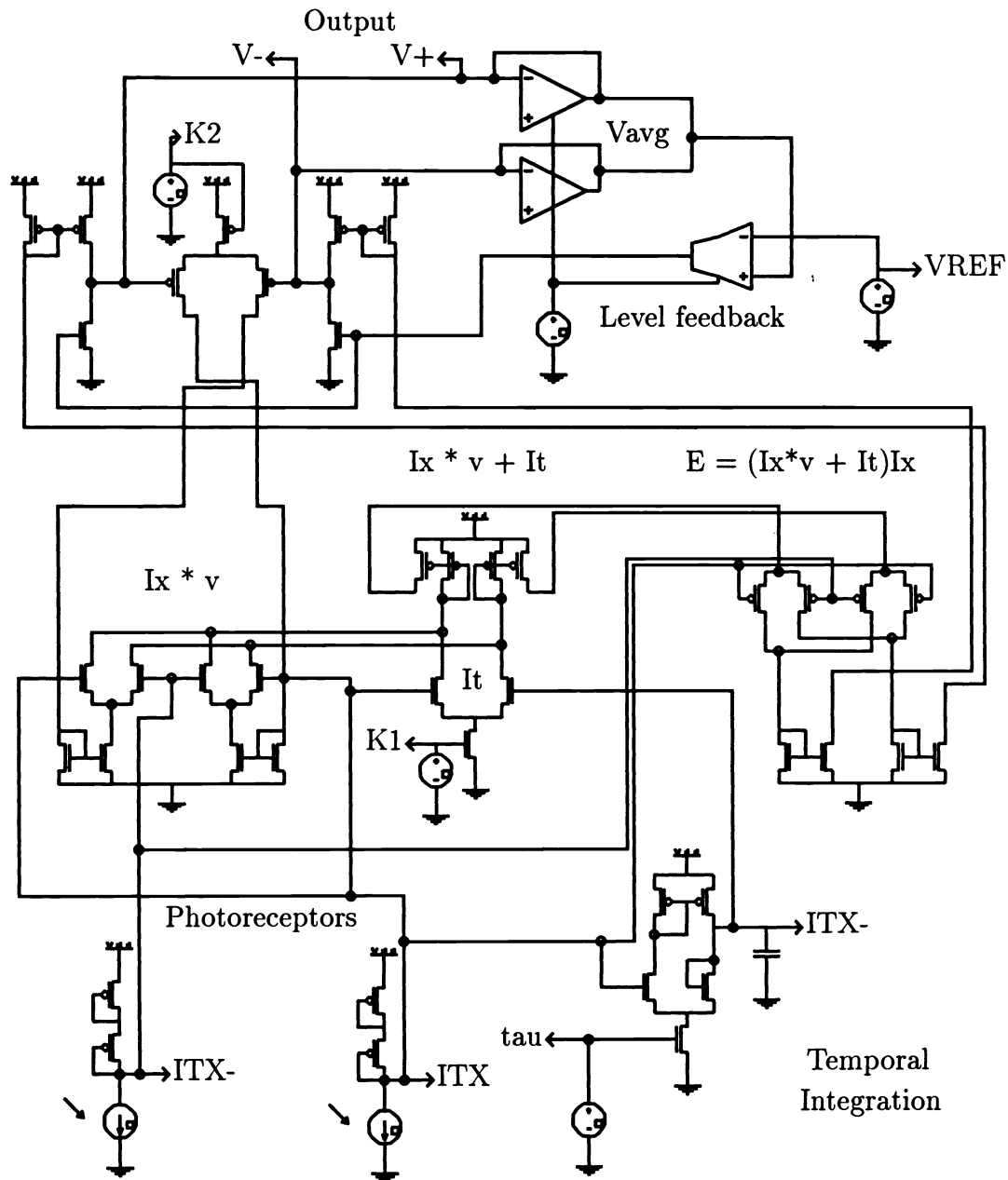


Figure 1. The motion detection circuit.

A current proportional to $I_x * v$ from the Gilbert multiplier at left is added at the top of the I_t differential pair, to form the sum $I_x * v + I_t$ as a sum of currents into a current mirror pair. The final weighting by I_x is carried out in the Gilbert multiplier at right; its output is a differential current proportional to the error signal $(I_x * v + I_t)I_x$.

The error current is mirrored twice; a voltage related to the error signal is developed by passing the mirrored current through a transistor that acts as a variable resistor. The level feedback circuit at top right insures that the differential voltage is symmetric about a reference level

(usually 2.5 Volts, since the power to the chip is normally supplied at 5 Volts). The voltage developed atop this variable resistor pair is the output of the chip; subtraction by an op-amp off chip gives a signal related to velocity. On the chip, this differential voltage is turned back into a differential current, and fed back as the velocity into the multiplier at bottom left. Negative feedback is accomplished by crossing the differential lines at the point of feedback.

3. OPENING THE LOOP

Three scaling constants in the motion detector circuit determine its range and mode of operation. $K1$ weights the time derivative I_t , $K2$ weights the error signal fed back as velocity, and τ sets the time constant for temporal differentiation. In terms of these parameters, the equation for the error signal is:

$$(e^{K2}I_x v + e^{K1}I_t(\tau))I_x = \epsilon. \quad (0.4)$$

It is evident that for $K1 \gg K2$ this expression reduces to a multiplication. The feedback loop is then broken, since the fed back value v has no effect on the error signal. This is the mode of operation explored in this paper.

4. PERFORMANCE FOR VARIOUS MOVING PATTERNS

The motion detection circuit operating as a multiplier was tested for moving stripes of various spatial frequencies at various light levels. We have fabricated and tested chips with many motion detection elements (computing an aggregate error signal) and chips with a single element.

Figure 2 shows the response of a single-element chip to moving high contrast stripes. At top are the outputs of the two photoreceptors; one has been moved down 1.5 Volts for clarity. The output at bottom is essentially zero for times when the stripe edge does not fall on the photoreceptors, and so the output is not a true velocity, but a spatio-temporal energy signal. The noisy character of the response is due to the level feedback, we believe.

Care was taken on this chip to prevent spatial aliasing: the two photoreceptors were laid out overlapping along the direction of motion and each photosensitive area describes the central lobe of the sinc function. While several portions of the biphasic sinc function are needed to keep the frequency content maximally compact, we believe that this is ample proof that the response is not due to spatial aliasing by the photoreceptors.

A signal linear in velocity may be obtained by integrating the spatio-temporal energy over time. For chips with a single element, this is achieved off-chip with an RC circuit with a long time constant (1-3 seconds, usually). For multi-element chips, the aggregation process itself performs some temporal integration; further integration off-chip may be used as well. The circuit operating as a multiplier, then, is largely a pulse generator which computes the correct sign of motion. For striped patterns, a pulse is generated at positive- and negative-going edges of the stripe. The faster the pattern moves, the more pulses are generated per unit time, and so integration over

time provides a measure of velocity.

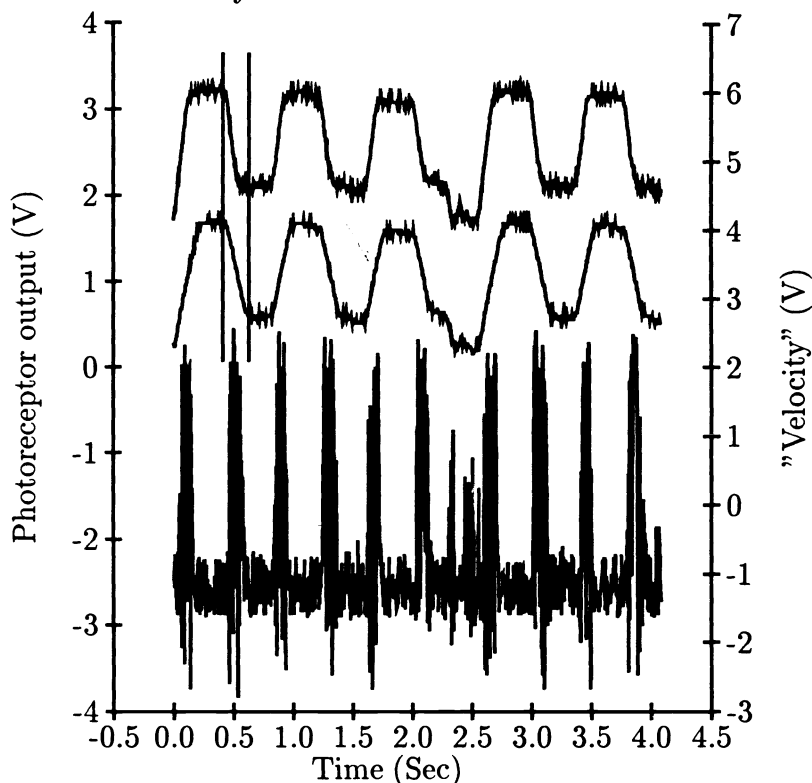


Figure 2. Response of a single element to moving stripes. The top two traces are photoreceptor outputs and the bottom trace is the product of the temporal and spatial derivative.

The response of the chip varies with light level for two reasons. First, the photoreceptor response itself varies with light level. As shown in Figure 3, both the AC and DC response to a moving stripe changes - the AC response increases and the DC level drops as the phototransistor pulls more and more current out of the pullup diodes. Second, since a transconductance amplifier saturates for differential voltages greater than about 200 mV, the follower integrator in the motion circuit will slew at step transitions greater than this amount. That is, the follower will become a current source, and the step input will be transformed to a ramp signal on the integrating capacitor. The difference between the input and the capacitor voltage forms the time derivative, and so I_t increases with light level. Most of the transitions in Figure 3 will cause slewing.

The consequence of this is shown in Figure 4. Here, the response of a single element is plotted for a range of velocities at three light levels: 7000 mW/m^2 (steepest curve); 100 mW/m^2 (intermediate curve); and 10 mW/m^2 (shallow curve). The response is fairly linear at a given illumination, and drops off (but remains linear) as the illumination is decreased. This drop-off is due to slewing in the time derivative computation. Perhaps more remarkable is that the chip can respond over nearly four orders of magnitude of illumination.

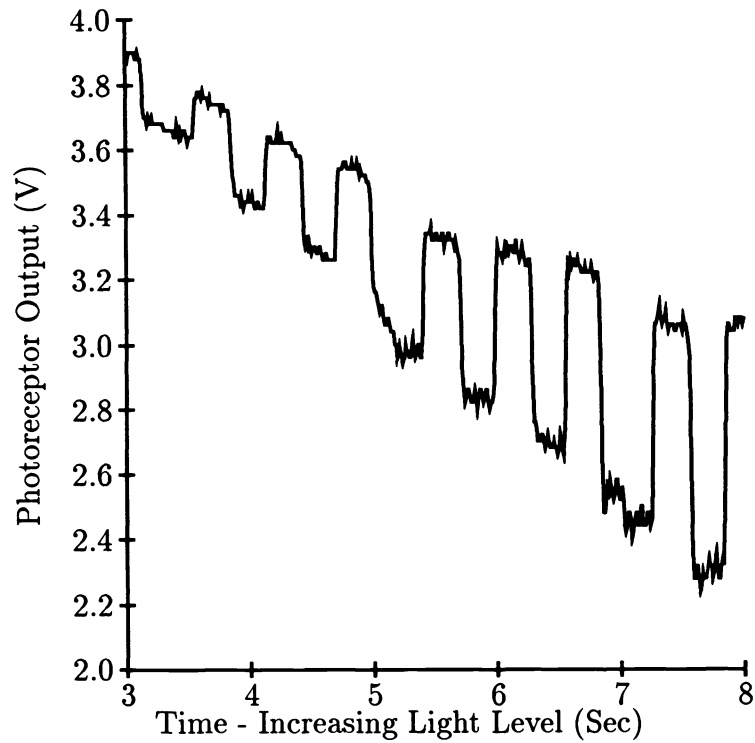


Figure 3. Variation of the photoreceptor output with light level.

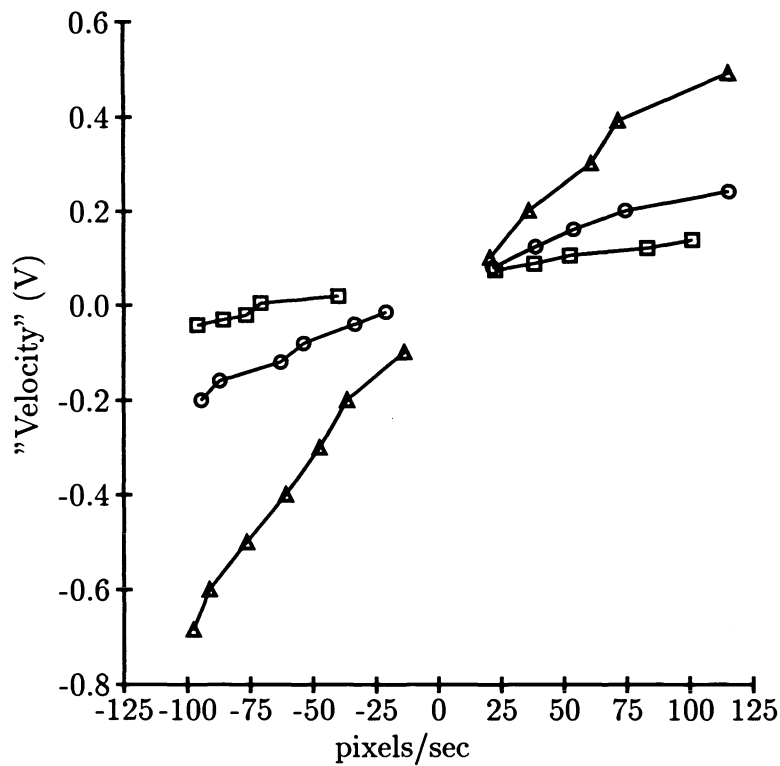


Figure 4. The integrated output of a single-element motion detector for various speeds and light levels. The light levels for the three curves are: steepest curve (triangles), 7000 mW/m^2 ; middle curve (circles), 100 mW/m^2 ; shallow curve (squares), 10 mW/m^2 .

Figure 5 shows the output of a chip with 30 elements computing an aggregate velocity. A motor is driving a wheel with stripes on its rim in view of the chip; the motor is powered with a current from a function generator set to produce slow triangle waves. The circuit is linear in pattern velocity - both positive and negative phases of the triangle wave are reproduced well. The common aggregation line serves to temporally integrate the outputs of the elements, smoothing over the noise evident in Figure 2 (no off-chip temporal integration is performed here). The velocity increase with light level is also demonstrated here. The photoreceptor AC output increases as a lamp is brought closer and closer to the wheel over a twenty second period. Mirroring this, the peak velocity output increases in time. (Dead zones in the velocity output are due to the motor threshold.)

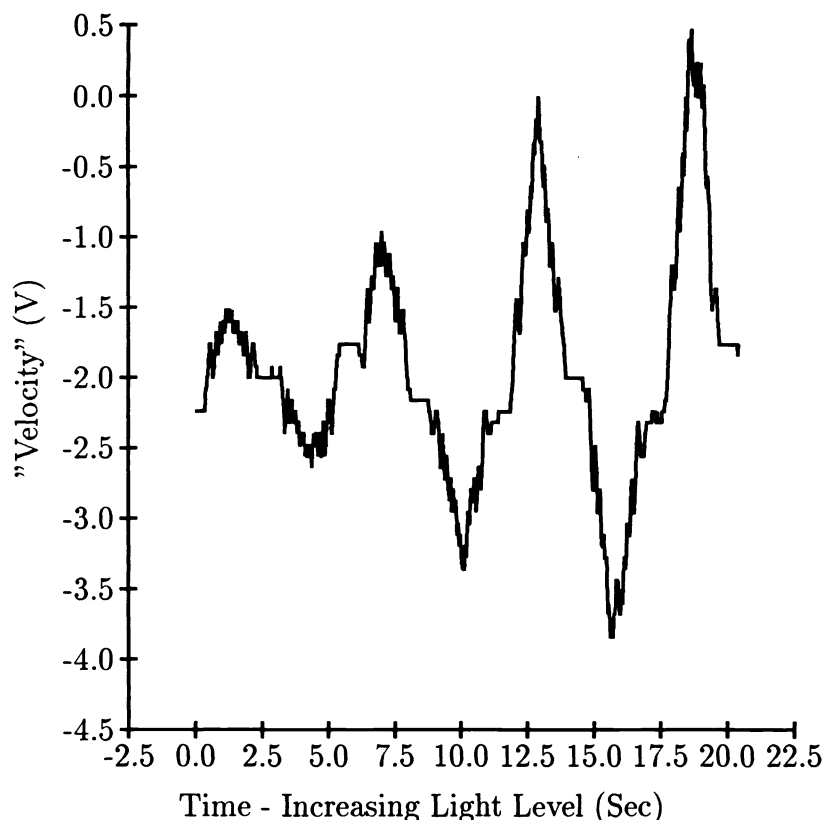


Figure 5. The response of a multi-element motion detection chip for a striped pattern whose velocity varies as a triangle wave, with light level increasing over time.

For a given light level, since the motion detection circuit responds with a signed pulse for a moving edge when operating in the multiplication mode, doubling the spatial frequency of a striped pattern doubles the pulse rate. A low-pass filtered version of the velocity output, then, should be linear in spatial frequency. Figure 6 shows this for high-contrast striped patterns at three spatial frequencies and a range of velocities. The patterns have a 50% duty cycle, so the relative spatial frequencies of the patterns with 1/4, 1/2 and 1 inch wide stripes are 4, 2, and 1, respectively. The slope roughly doubles from the 1 inch to 1/2 inch patterns and from the 1/2 inch to 1/4 inch patterns. This data was taken from a multi-element chip and so its output is the aggregate (sum) of the error signals from its elements. The summation saturates fastest for the

highest frequency, later for the middle frequency, and does not saturate for the lowest frequency pattern at the highest available test velocity.

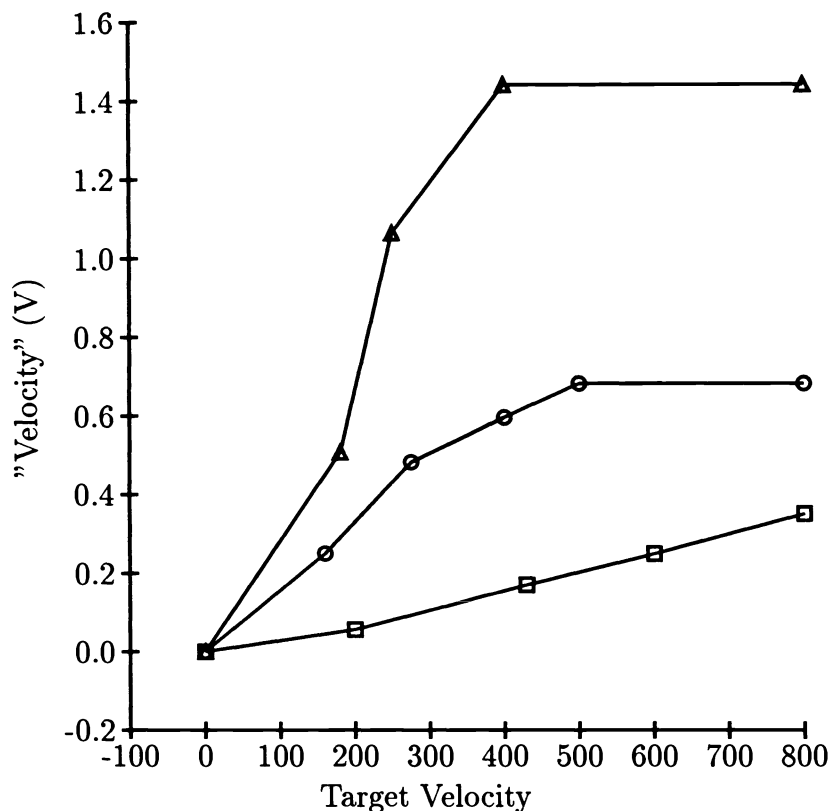


Figure 6. The output of a multi-element motion detection chip for striped patterns of different spatial frequencies: triangles, 1/4 inch stripes; circles, 1/2 inch stripes; squares, 1 inch stripes. The output is roughly linear in spatial frequency.

5. APPLICATION TO THE TIME-TO-CONTACT PROBLEM

A well-known phenomenon in the psychophysics of early vision is the *time to contact* behavior. Flies, birds, and human long jumpers are thought to use the rate of looming of an image on their retina to judge the time to collision. Flies extend their legs for landing when the surface they are approaching looms in their visual field. It is the rate of looming, independent of the size of the target, that triggers the landing behavior⁵. Gannets, an avian species that dive for fish in the firths of Britain, seem to use the same measure, the rate of looming of the surface of the water, to trigger retraction of their wings before plunging into the water⁶. Further up the evolutionary scale, human long jumpers apparently fixate on the take-off board as they run toward it, and accurately judge the distance for their final step before jumping via the rate of looming of the board⁷.

A very low order measure of the rate of looming is a thresholded velocity. A time-to-contact scenario was thus constructed in the following way. A multi-element motion detector chip, operating in the multiplication mode, was pointed at one side of a rotating card. The velocity of

the edge of the card, in projection, is sinusoidal, with peak velocities when the card is parallel to the line of sight and zero velocity when the card is perpendicular to the line of sight (i.e., fronto-parallel). As shown in Figure 7, the chip output is indeed sinusoidal. A threshold set at an arbitrary positive velocity represents the velocity that is the critical looming rate.

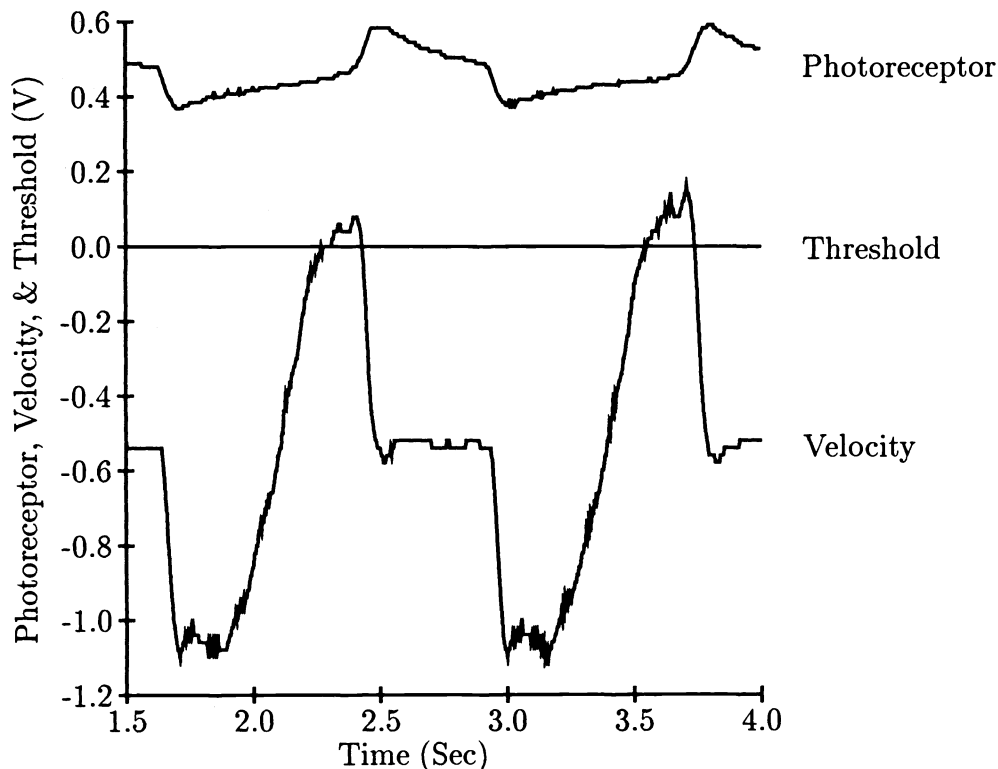


Figure 7. The output of a multi-element motion detection chip viewing the right half of a card rotating about a vertical axis; the line of sight is horizontal. The motion, which is sinusoidal in the perspective projection, is captured well by the chip. In a time-to-contact scenario, positive velocities represent looming. A threshold of the positive velocity provides a primitive estimate of time to contact.

6. CONCLUSION

A novel mode of operation of an integrated optical motion detector was explored under a variety of conditions. The main problems with this chip are the variation in motion output with light level and contrast and the very fact that this mode of operation must be used when the chip is used on arbitrary images. Variation of the chip output with spatial frequency derives from its mode of operation.

These problems could be solved in two ways. First, the range of the differential pairs throughout the circuit should be widened. We have in a fabrication a new design that may accomplish this. Second, and more critical in our opinion, a more sophisticated photodetector should be incorporated in this circuit. DC level clamping and AC gain control at the photoreceptor level would eliminate the variation in velocity output with light level and would extend the sensitivity

to lower contrasts. Indeed, with a better input, this circuit would be able to operate as originally intended and so spatial frequency dependence would be eliminated.

7. ACKNOWLEDGEMENTS

We are grateful to John Tanner and John Harris for helpful discussions, to Carver Mead for support and encouragement, to Hewlett-Packard for computing support in the Mead lab, and to DARPA for MOSIS fabrication services. A.M. was supported by fellowships from the Parsons Foundation and the Pew Charitable Trust and by research assistantships from Office of Naval Research, the Joint Tactical Fusion Program, the Center for Research in Parallel Computation, and the Program in Advanced Technologies, which was sponsored by General Motors and TRW. We gratefully acknowledge support from the Hughes Aircraft AI Research Lab and the Rockwell International Science Center for chip efforts in the Koch lab.

8. REFERENCES

1. J. Tanner and C. Mead, "An integrated optical motion sensor," *VLSI Signal Processing II*, S-Y. Kung, R.E. Owen, and J.G. Nash, eds., 59-76, IEEE Press, NY, 1986.
2. J. Tanner, *Integrated optical motion detection*, Ph.D. Thesis, California Institute of Technology Dept. of Computer Science, 1986.
3. J. Tanner and C. Mead, "Optical motion sensor," *Analog VLSI and Neural Systems*, C. Mead, 229-255, Addison-Wesley, Reading, MA, 1989.
4. B.K.P. Horn and B.G. Schunck, "Determining optical flow," *Artificial Intelligence*, vol. 17, 185-203, 1981.
5. H. Wagner, "Flow-field variables trigger landing in flies," *Nature*, vol. 297, 147-148, 1982.
6. D.N. Lee, "The optic flow field: the foundation of vision," *Phil. Trans. R. Soc. Lond. B*, vol. 290, 169-179, 1980.
7. D.N. Lee, "Plummeting gannets: a paradigm of ecological optics," *Nature*, vol. 293, 293-294, 1981.